Engineering and Technology Journal e-ISSN: 2456-3358
Volume 05 Issue 03 March-2020, Page No.-676-691
DOI:10.33826/etj/v5i3.01, I.F. – 6.127

Removal of Zinc in an Aqueous Solution by Kaolin Kinetic and Thermodynamic Studies

Toufik CHOUCHANE[1], A. BOUKARI[2]

[1,2] Research Center in Industrial Technologies CRTI, P.O.Box 64, Cheraga 16014 Algiers Algeria

Abstract: In this work, the physico-chemical characterization showed that the adsorbent consists mainly of silica and alumina and its structure is disordered. The specific surface area measured is more considerable for purifying and activated kaolin. The point of zero load is measured at pH 6.6.The envisaged process is in batch systems. The results of the tests carried out indicate that the equilibrium is reached after 30 minutes. This sorption is maximum at 20°C, for stirring speed of 150 rpm, particle size between 150 and 200 µm and a pH 4.3. The maximum adsorption capacity is 39.9 mg/g. The kinetic study shows that the adsorption of zinc by kaolin follows the pseudo-first order kinetics and the Langmuir model is the most appropriate. In the same context, the results indicate a highly favorable adsorption of zinc on the kaolin($0 < R_L < 1$). Thus, application of the diffusion model informed that the external transport seems to be a step controlling the overall speed of the process while the intra-particle diffusion is involved in the overall rate of sorption process but this is not the only step that controls the speed.The thermodynamic parameters show that the adsorption of Zn on kaolin is spontaneous, exothermic and that randomness decreases at the interface during adsorption.

Keywords: kaolin, zinc, adsorption, kinetics, water treatment.

1. Introduction

The pollution of water by toxic metals can create health risks for humans and their environment[1]. The control of this pollution type demands the implementation of specific processes of treatment. Among these, we find ion-exchange[2], solvent extraction[3], reverse osmosis[4], ultrafiltration[5] and adsorption[6,7].Then it required the utilization of others efficient and low cost adsorbents. In this case, we have oriented our study on the elimination of metallic ions with a low-cost material namely Kaolin of Guelma as an adsorbent. The use of kaolin as adsorbent is intended to implement a method of water treatment by adsorption, in particular for the treatment of colored water[8-11], the elimination of organic molecules[12-14] and the adsorption of toxic metals[15-18] contained in wastewater.

We have chosen the zinc as metal representing the heavy metals contained in wastewaters. It's elimination from the aqueous medium is envisaged in static mode. The zinc solutions were prepared from zinc nitrate dissolved in bi-distilled water. Some parameters influence the amount of metal ions being removed by kaolin; initial zinc concentration, agitation speed, pH, temperature and particle size of the solid. Optimization of these parameters is able to improve the capacity of solid adsorption, then made it possible to study the effect of every parameter. The isotherms, the kinetics and the adsorption mechanism can inform us about the quality of the process.

2. Materials and Methods

2.1 Materials

The kaolin is a hydrothermal rock obtained from Djebel Edbagh of Guelma (east of Algeria). This kaolin is characterized after milling and sieving of powder which have a particle size below 300 µm and followed by two washings. The first wash is done from a solution based on sodium chloride. It consists to eliminate all the crystalline phases[19,20]. This treatment is follow eddirectly by other washings with bi-distilled water to remove the residual salts[21] followed by filtration [22]. The obtained powder was dried during 24 hrs under vacuum at 105°C. Further, all reagents used in the preparation of adsorbent materials such as HCl, zinc nitrate were obtained from Merck produce in analytical grade.

2.2 Analytic methods

The zinc concentration was measured by atomic absorption spectroscopy method [23] using PerkinElmer 3110 equipments associated with hollow cathode lamp monolayer and oxidizing flame provided by mixed air-C_2H_2 and device coultornic Micrometrics 2100 E. The pH solution was adjusted with Ericsson pH meter. The characterization was carried out by FRX (Siemens SRS 3000) and DRX (Rigaku Ultim IV). The morphology was observed using a scanning electron microscope (Zeiss EVO MA25). The specific surface area was measured by BET method [24].

2.3 Adsorption experiments

A series of batch experiments were conducted to study the adsorption mechanism of zinc onto kaolin, adsorption isotherms, adsorption kinetics and thermodynamic parameters.

The adsorption experiments are realized by adding an amount 1 gr of prepared kaolin to an aqueous solution containing zinc ions. The zinc solutions were prepared from zinc nitrate ($Zn(NO_3)_2$, $6H_2O$)dissolved in bi-distilled water. The continuous mixing was ensured during the experiment with a constant stirring speed using a mechanical agitator. The temperature was controlled with water bath shaker. The pH solution was fixed in desired value by adding a few drops of concentrated ammonia. The adsorption kinetics were followed by sampling of 5 ml every 5mins.

2.4 Operating conditions

The operating conditions used in this process are represented as follows:

- Determination of equilibrium time: $C_{initial}$: 30 mg/L; $V_{agitation}$: 100 rpm; pH: 5,4;T: 20 °C; granulometry: $150 \leq Ø_{kaolin} < 200$ µm; M_{kaolin} : 1 g .
- Optimization of the agitation speed of the medium: $C_{initial.}$: 30 mg/L; $V_{agitation}$: 50,100, 150, 200 rpm; pH: 5,4; T: 20 °C; granulometry: $150 \leq Ø_{kaolin} < 150$ µm; M_{kaolin} : 1 g.
- Optimization of temperature:$C_{initial.}$: 30 mg/L; $V_{agitation}$: 150 rpm; pH: 4,3;T: 20, 30, 40, 60°C; granulometry: $150 \leq Ø_{kaolin} < 200$ µm; M_{kaolin} : 1 g.
- Optimization of the solid particle size: $C_{initial.}$: 30 mg/L; $V_{agitation}$: 150 rpm; pH: 4,3; T: 20°C; granulometry: $Ø_{kaolin} < 100$ µm, $100 \leq Ø_{kaolin} < 150$ µm, $150 \leq Ø_{kaolin} < 200$ µm; $200 \leq Ø_{kaolin} < 300$ µm, M_{kaolin} : 1 g.
- Measurement of the maximum absorbed capacity: $V_{agitation}$: 150 rpm; pH: 4,3; T: 20 °C; granulometry: $100 \leq Ø_{kaolin} < 150$ µm; M_{kaolin} : 1 g.
- Adsorption isotherm: $V_{agitation}$: 150 rpm; pH: 4,3;T: 20 °C; granulometry: $100 \leq Ø_{kaolin} < 150$ µm; M_{kaolin} : 1 g.

3. Results and Discussion

3.1 Characterization of kaolin

The physical and chemical characteristics of the kaolin studied were obtained after grinding, sieving of the particles below 40 µm and degaussing under vacuum at 105 °C for 12 hours.

The chemical composition of kaolin is reported in Table 1, where we found a dominance of Al_2O_3 and SiO_2 of the order of 82.02%. The remaining oxides are divided into two categories. Those which have a low percentage by mass (Fe_2O_3, MnO, TiO_2) and those which are in trace form (MgO, CaO, NaO_2). A loss on ignition of 13.55%.

Table 1. Chemical composition of Djebel Edbagh kaolin

Elements	SiO_2	Al_2O_3	Fe_2O_3	MnO	MgO	CaO
% Mass	46.58	36.82	0.730	Trace	Trace	Trace
Elements	NaO_2	K_2O	TiO_2	LI	H_2O	
% Mass	Trace	0.051	0.029	13.55	1.43	

X-ray diffraction analysis allows the nature characterizing of crystallized mineral phases present in the kaolin Figure 1 shows the diffractogram of the raw kaolin sample. The results of this test show that the kaolin of Guelma contains kaolinite and quartz, where we note intense peaks of kaolinite. This observation justified the results obtained by X-ray fluorescence.

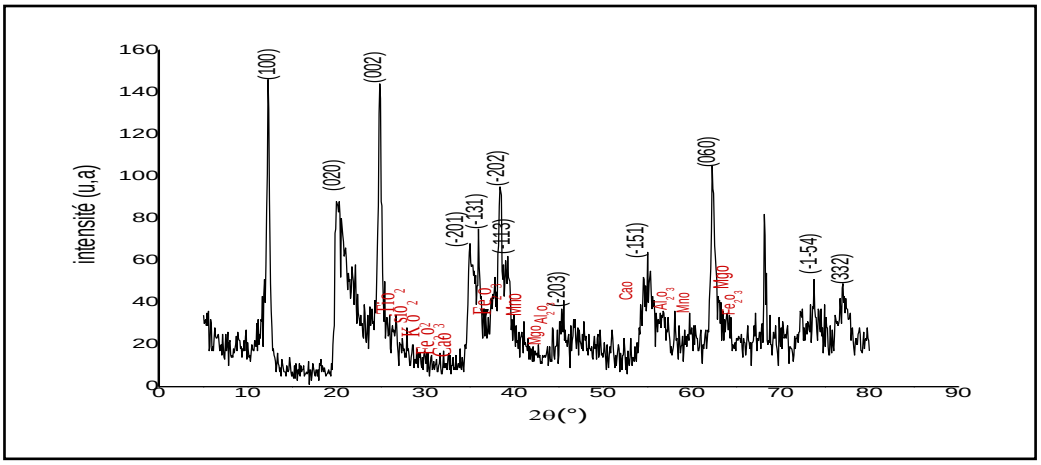

Figure 1. Diffractogram of raw kaolin

The morphologies of both the raw kaolin and the kaolin after purification and activation are determined by scanning

electron microscope. The obtained results are shown in Figures 2 and 3. From these pictures, we note hexagonal faces that are difficult to observing it and also we note a disorder in the distribution of the pores (structures upset). For the Figure 2, we notice the presence of new sites caused by the activation of the kaolin.

The specific surface area of the kaolin raw, purified and purified then chemically activated, was determined experimentally in the laboratory by BET method. The purified, then chemically activated showed a high specific surface equals 74.4 $m^2.g^{-1}$ compared to purified kaolin and raw kaolin, which showed the following specific surface values respectively: 31.4 and 13.5 $m^2.g^{-1}$.

Determination of point zero charge is an analytical method which has been the subject of several studies[25,26]. The pH point zero of charge is the pH value of the solution surrounding the adsorbent when the sum of surface positive charges is equal to the sum of surface negative charges[27].The point of zero charge (pH_{PZC}) is determined by the method of P. Chutia et al.[28]. For the kaolin studied, the pH_{PZC} is 6.6.

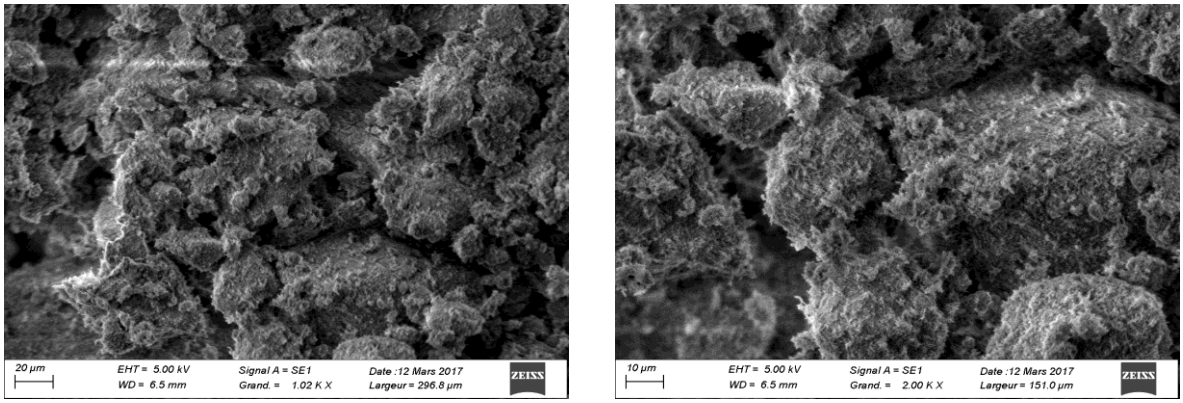

Figure 2.SEM picture of raw kaolin of djebel Debagh / Guelma

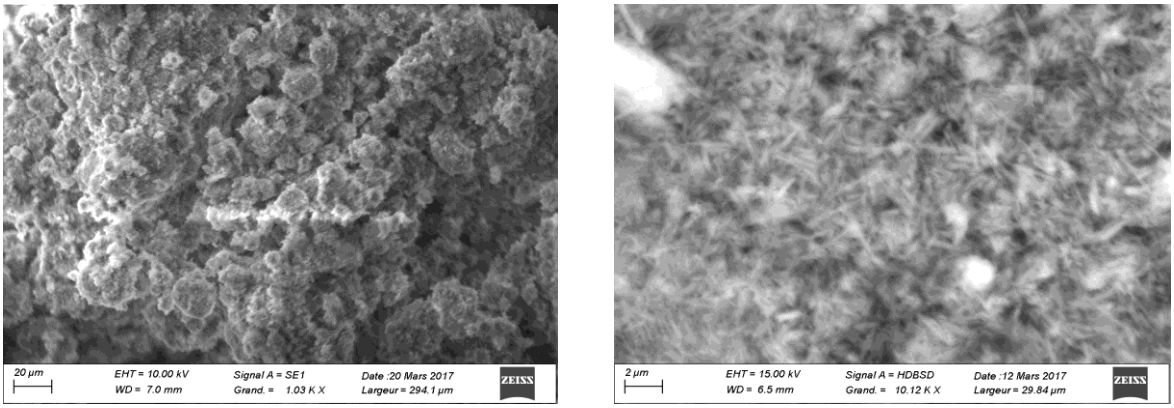

Figure 3. SEM picture of activated of djebel Debag / Guelma

3.2 Effect of agitation time

The influence of contact time on the adsorption of zinc in solution by kaolin was studied at various initial concentrations: 10, 20 and 30 mg/L. From figure 4, we notice the increased agitation time increased the uptake of zinc with maximum adsorption was observed after 30 min. Beyond this time, the residual concentration becomes almost constant. This means that the adsorbent has reached the saturation phase. for this purpose, we consider this duration as the equilibrium contact time.

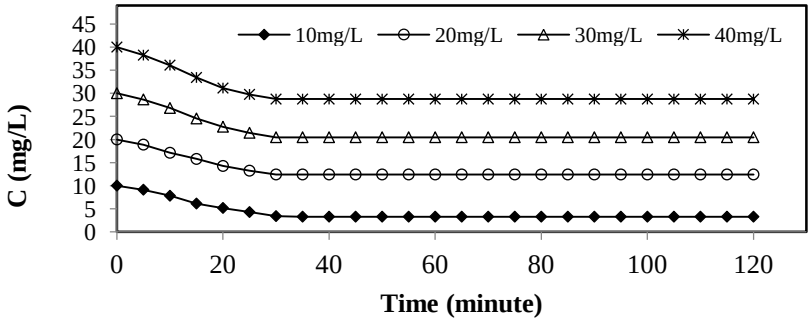

Figure 4. Residual concentration of Zn^{+2} as function of time: Effect of agitation time

3.3 optimization of influencing parameters

The optimization of the influencing parameters is an indispensable step in the adsorption processes. It allows us to study the kinetics of adsorption in order to optimize the parameters influencing and to determine the maximum quantity adsorbed by the solid.

3.3.1 Effect of stirring speed

The influence of stirring speed is an important factor in this adsorption process. In fact, it contributes to the distribution of the adsorbate in the adsorbent and the determination of the maximum adsorbed quantity[29].

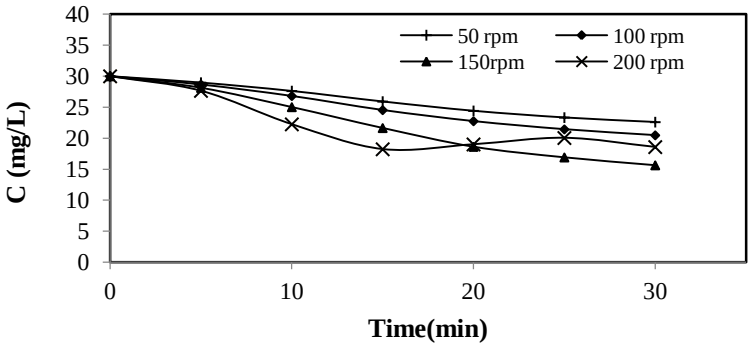

Figure 5. Residual concentration of zinc as function of time: Effect of stirring speed

In this work, the speeds are fixed between 50 and 200 rpm (Fig. 5,6). Figure5 show that the zinc quantity adsorbed by the kaolin increases with the increase of stirring speed until 150 rpm. For a speed of 200 rpm, We observe fluctuations in residual zinc concentration values. This phenomenon is probably due to the return of the ions from the solid to the solution[30].

Following these experimental results, we consider 150 rpm the optimal stirring speed and we conclude that the stirring speed contributes greatly in the transfer of zinc from the solution to the adsorbent which gives it an important role in external transport[31].

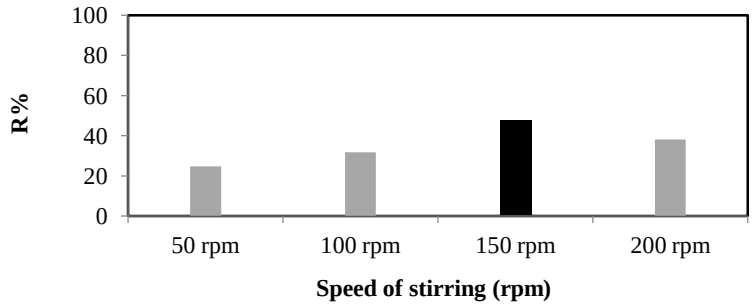

Figure 6. Zinc removal efficiency as function of stirring speed

3.3.2 Effect of pH

The pH of the solution is an important parameter in the adsorption phenomenon because it affects the form of metal in solution, as well as the surface properties of the adsorbent[32-35].

In this work, the pH range of the explored medium is ranges from 2.5 to 6 (Fig. 7). The effect of the pH of the solution shows that at pH 2.5 the adsorption of the zinc on the solid is unfavourable(Fig.7,8). Indeed, for a strongly acidic medium (pH 2.5), the proton excess slows the transfer of ion from the solution to the adsorbent[36,37].

we notice that the capacity of adsorbed zinc has increased remarkably as the solution pH increased from 2.5 to 4.2. Indeed, in this pH range, the yield increased from 18.63 to 62.83% (Fig. 7,8). The efficiency of adsorption can be explained by the effect that the pH of the solution has favorably influenced the surface charges of adsorbent[38].

For the high pH values, the adsorption of zinc is less important and begins to decrease as the pH increases. The residual measured concentration and the calculated yield are respectively: 15.64 mg/L, 18.74 mg/L and 47.86%, 37.73%. This phenomenon can be explained by the surface charge of adsorbent. given that the net charge of the adsorbent is zero at pH 6.6.

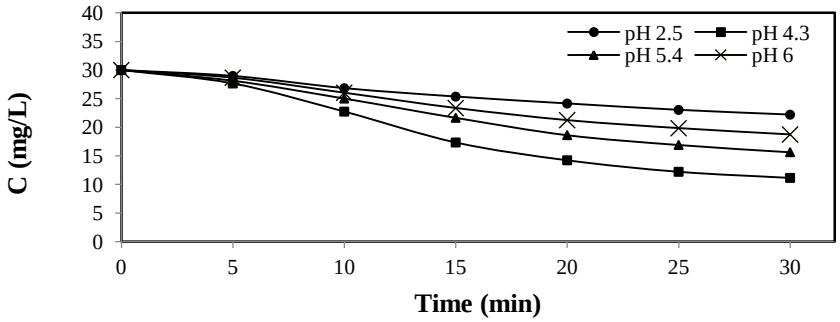

Figure 7. Residual concentration of zinc as function of time: the influence of pH

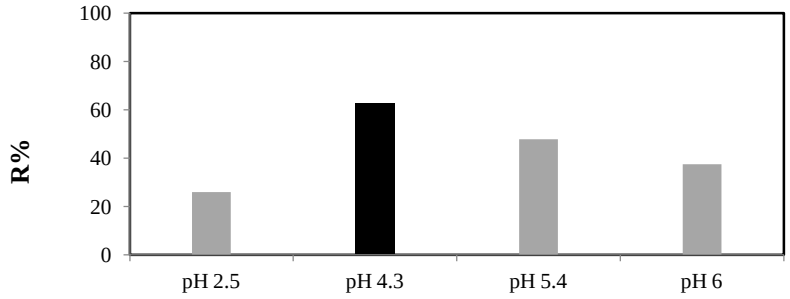

Figure 8. Zinc removal efficiency as a function of pH

3.3.3 Effect of temperature

The temperature of the medium is very important influencing parameter affecting the fixation of metal on the adsorbent because it exerts a considerable influence on the sorption rate [39-41]. The temperatures studied in this work are varied from 20 to 60 °C (Fig. 9).

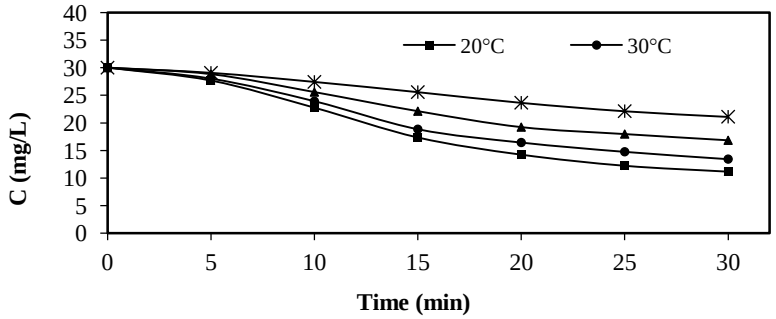

Figure 9. Residual concentration of zinc as a function of time: the influence of temperature

The study of the temperature influence on the zinc adsorption by kaolin in solution shows the tan inverse relationship between temperature and quantity of adsorbed ion (Fig. 9,10). Indeed, the results showed clearly that the fixation of zinc is more important at 20 °C and the adsorbed quantity begins to decrease from 30 °C (Fig. 9,10). The inefficiency of zinc adsorption with temperature rise is due to the destruction of the active binding sites, or the weakening of the attraction bonds between the adsorbate and the adsorbent[42]. This result also explains that the sorption of zinc in aqueous medium on the kaolin is exothermic[43].

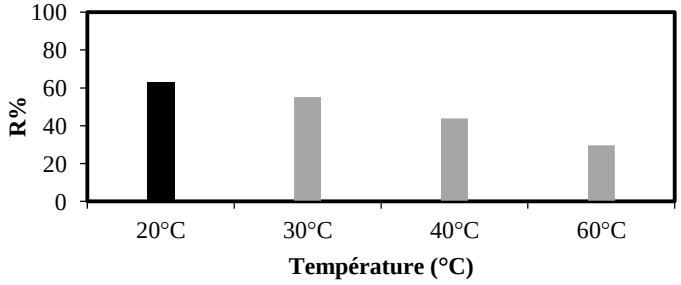

Figure 10. Zinc removal efficiency as a function of temperature

3.3.4 Influence of particles size of kaolin

The particle size of the adsorbent has a predominant role in the rate of transfer of the cation from the solution to the adsorbent[44-46]. In this context, we have optimized the particle size of kaolin using diameters vary from 100 to 300 µm (Fig. 12). From these results we can see that the best obtained yields are that for the kaolin particle size of 100 ≤ Φ < 150 µm (Fig. 11). The previous tests reveal that the absorption of zinc on the kaolin for diameter Φ<100 µm is considered unfavourable (Fig. 11,12).

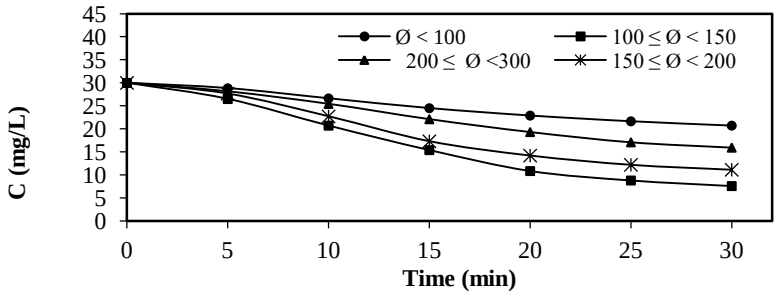

Figure 11. Residual concentration of zinc as function of time: influence of the granulometry

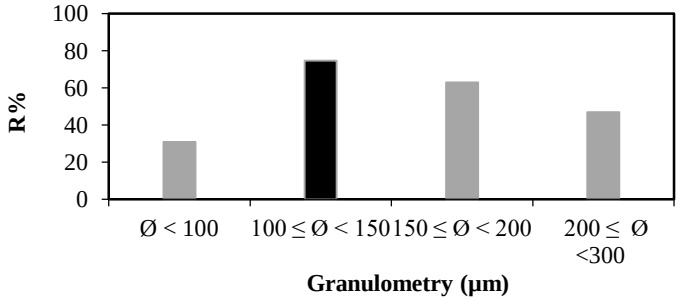

Figure 12. Zinc removal efficiency as a function of particle size of kaolin

3.3.5 Effect of chemical activation of kaolin

To improve the adsorption efficiency by creating other sites, we have activated the surface of our solid using ahydrochloric acid[48-50]. The experimental measurements showed that the optimal concentration of acid giving the best zinc fixation is 0.2 M (Fig.13).

After activation of the kaolin by 0.2 M hydrochloric acid and by applying all the optimized parameters, we can see a decrease in the residual zinc concentration until 2.81 mg/L at equilibrium (Fig. 13) corresponding to an increase in the yield value of 13.1% (Fig. 14).

The activation of kaolin by hydrochloric acid would probably increase the number of sites then favored the process of fixing of metal ions on its surface.

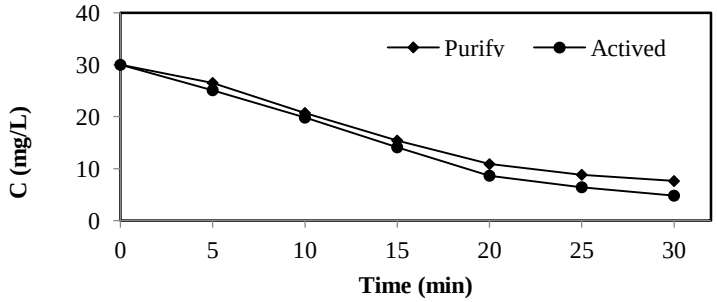

Figure 13. Residual concentration of zinc as a function of time

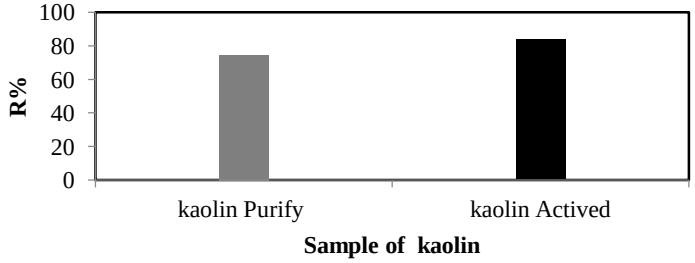

Figure 14. Yield of zinc adsorption for treated kaolin

3.3.6 Effect of initial concentration

The removal of zinc by kaolin in synthetic solutions [10, 20, 30, 40, 50, 60, 70, 80 mg/L] was carried out under the abovementioned optimum conditions. The maximum amount adsorbed at equilibrium was determined using the residual method (eq.1)[51,52].

$$q_e = \frac{C_0 - C_e}{m} \times V \quad (1)$$

Where: C_0 is Initial solute concentration (mg/L); C_e is the residual solute concentration at equilibrium (mg/L); m is the mass of the adsorbent and V is volume of solution.

The adsorption isotherm of zinc at the surface of the solid is obtained by plotting the adsorbed amount as a function of initial concentration at equilibrium (Fig. 15). The obtained curve showed that the adsorbed amount are increased with increasing of initial concentration until a certain threshold. The value of the amount adsorbed at this level is: 39.39mg/g. This result allows us to conclude that this quantity represents the maximum quantity which can be fixed by one gram of kaolin.

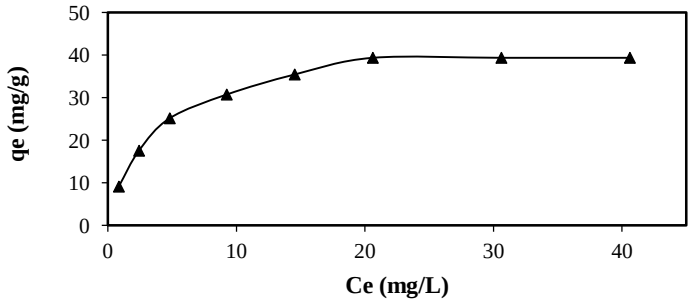

Figure 15. Adsorbed amount of zinc based on the initial concentration

3.4 Adsorption isotherms

to describe the adsorption phenomenon and explicate metal ion–clay interaction, we used two frequently employee models in this case the Langmuir and Freundlich isotherms.

The Freundlich equation is well adapted to describe the equilibrium in aqueous phase [53]. Its empirical formula is:

$$q_e = \frac{x}{m} = K_F C_e^{\frac{1}{n}} \quad (2)$$

Where q_e is the amount of adsorbent fixed at equilibrium by the adsorbent(mg g^{-1}), C_e is the residual concentration at equilibrium (mgL^{-1}) ; K_F and 1/n are the Freundlich constants related to adsorption and affinity. The linearized Freundlich relation is written as follows:

$$\log q_e = \log K_F + \frac{1}{n} \log C_e \quad (3)$$

The Langmuir equation[54], derived from kinetics where equilibrium arguments are commonly applied to chemisorption of gases, is expressed in the case of adsorption in solution:

$$q_e = \frac{b q_{max} C_e}{1 + b C_e} \quad (4)$$

Where q_e is the amount of adsorbent fixed at equilibrium by the adsorbent(mg g^{-1}), C_e is the residual concentration at equilibrium(mg L^{-1}), q_{max} is the maximum saturation capacity of the adsorbent(mg g^{-1}) and b is the thermodynamic constant of the adsorption equilibrium ($L.mg^{-1}$). The linear form of the Langmuir equation is shown below (Eq.5):

$$\frac{C_e}{q_e} = \frac{1}{q_{max}} C_e + \frac{1}{q_{max} b} \quad (5)$$

In this work, Langmuir and Freundlich isotherm models are used to fit the equilibrium adsorption data. The obtained plots are represented by Figures 16 and 17. The parameters of these equations are reported in Table 2. From the obtained results, the Langmuir model is more suited to this adsorption than that of Freundlich model. This result is justified by the values of the regression coefficients and the maximum adsorbed quantities (Table 2).

Table 2. Isotherm parameters for adsorption of zinc by kaolin

Modèle Freundlich			Modèle de Langmuir		
K_F $(mg.\ g^{-1})(ml.mg^{-1})^{1/n}$	n	R^2 (%)	q_{max} (mg/g)	B $(L.mg^{-1})$	R^2 (%)
11.88	3.03	0.92	40.81	0.326	0.99

According to the value of the Freundlich parameter n (1 > n > 10), we conclude that the adsorption process is favorable [55]. Figure 18 shows the zinc adsorption isotherm by kaolin of Guelma in aqueous solution. The adsorption isotherm has a classical isotherm type I. The saturation of the adsorption sites takes place gradually until a plateau of saturation is reached. The maximum adsorbed amount is 39.39 mg/g. The presence of a plateau indicates a weak formation of the multilayer (Fig. 18)[56,57]. Consequently, the Langmuir equation gives a better representation of the zinc adsorption isotherm by kaolin.

The parameters of the Langmuir model can even be used to

establish the affinity between adsorbent and adsorbate, this Affinity is determined by the ratio R_L[58,59]. R_L is a unitless quantity indicating whether the adsorption is more favorable as R_L tends to zero and more unfavorable as R_L tends towards 1[60,61].

The ratio is calculated as a function of the Langmuir constant and the initial concentration values as follows (Eq.6):

$$R_L = \frac{1}{1+C_0 b} \quad (6)$$

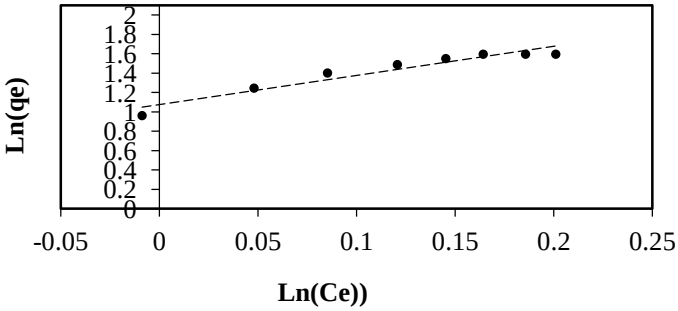

Figure 16. Presentation of Freundlich model

Where R_L: the Ratio indicates the quality of the adsorption, b is the Langmuir isotherm constant and C_0 is the initial concentration of solution. As the Figure 19, we observed that the values of R_L as a function of the initial concentration are between 0 and 1. Thus confirm the favorable nature of the adsorption and indicate that the solid has a high adsorption capacity.

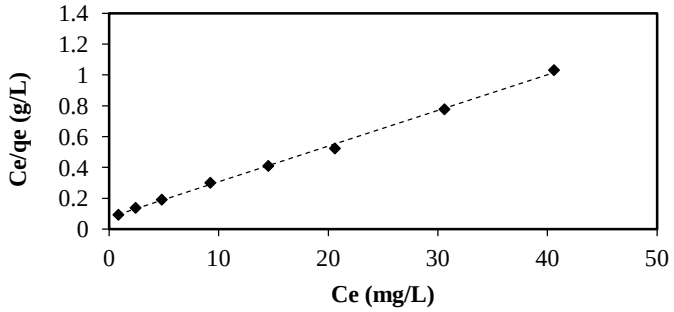

Figure 17. Presentation of Langmuir model

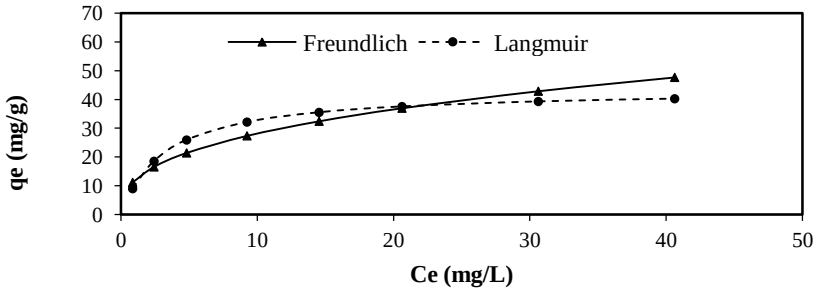

Figure 18. Adsorption isotherm of zinc on kaolin

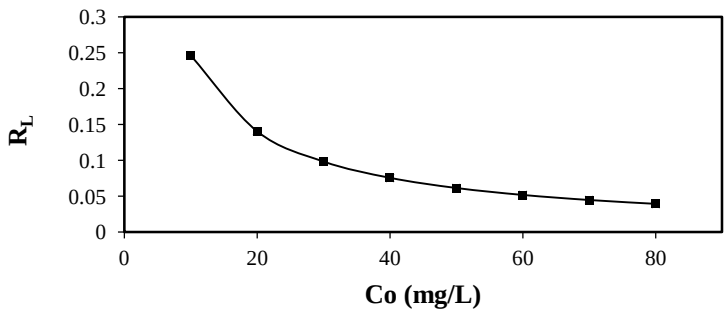

Figure 19. R_L as function of zinc initial concentration

3.5 Kinetics of adsorption

Monitoring the kinetics is an important step in the adsorption. The adsorption of the heavy metals from the liquid phase to the solid phase can be considered as a reversible reaction at equilibrium being established between the two phases[62]. The order of the reaction was determined on solutions of different concentrations, namely 30, 40 and 50 mg/L. These tests were carried out under the optimum conditions. The pseudo order of the reaction is calculated by the two kinetic models: the Lagergren model and the Blanchard model.

3.5.1 Pseudo first order

The Lagergren relation[63] focused on the adsorbed amount is the first-rate equation established to describe the sorption kinetics in a liquid-solid system. This pseudo first order model is represented by the following relation:

$$\frac{dq}{dt} = k_{Lag}(q_e - q) \quad (7)$$

The integration of Equation 7 for boundary conditions: q= 0 à t= 0 et q= q à t= t :

$$ln\frac{q_e - q}{q_e} = -k_{Lag}t \quad (8)$$

Where q_e is the adsorbed quantity at equilibrium (mg/g), q is the adsorbed quantity at time t (mg/g), t is Time of adsorption process in this study it is from 0 to 30 minutes, k_{Lag} is the constant pseudo first order sorption speed(s^{-1}).

$$\ln(q_e - q) = -k_{Lag}t + lnq_e \quad (9)$$

If the relation of Lagergren is satisfied by carrying ln (qe-q) as a function of time t, we must obtain a straight line with a slope -k and an ordinate at the origin equal to ln (qe) [64].

In this case, the correlation coefficients must be $R_2 \geq 0.9$ and the values of the theoretically determined maximum sorption capacity at equilibrium are close to the experimental values[65,66].

Table 3. Parameters kinetic of Lagergren models

C_0 *(mg/L)*	$K_{lag.}$ *(g/mg.min)*	$q_{etheo.}$ *(mg/g)*	$q_{eexp.}$ *(mg/g)*	R^2 *(%)*
30	0.128	28.46	25.19	95.8
40	0.123	32.14	30.76	97.5
50	0.119	37.22	35.74	97.1

The plots of ln (q_e-q) curves as a function of time are shown in Figure 20 and the parameters of the Lagergren model are given in Table 3. According to Table 3, we note that the regression in all three cases is greater than 90% and the maximum theoretical and experimental adsorbed capacities are close for the three media used.

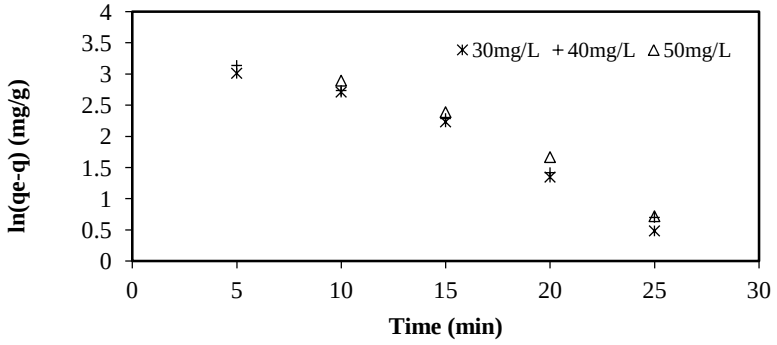

Figure 20 . Pseudo first order kinetic

3.5.2 Pseudo second order

The application of the Blanchard model[67] allows us to define the pseudo-second order of the reaction in a sorption process. it is presented in the following form (éq.10):

$$\frac{dq}{dt} = k_b(q_e - q)^2 \quad (10)$$

(10)

Where q_e is the adsorbed quantity at equilibrium (mg/g), q is the adsorbed quantity at time t (mg/g), t is Time of adsorption process in this study it is from 0 to 30 minutes, k_b is the constant pseudo second order sorption speed(min^{-1}).

By integrating equation 10 and applying the boundary conditions we obtain the following :

$$\frac{t}{q} = \frac{1}{k_b q_e^2} + \frac{1}{q_e} \quad (11)$$

By taking t / q as function of time t, we will have to obtain a straight line of slope 1 / q_e and ordinate at the origin 1 / k_b. qe^2. The Blanchard model is verified only if the correlation coefficients R ≥ 0.9% and the theoretical and experimental maximum capacities are close [68,69].

Table 4. Parameters kinetic of Blanchard model

C_0 *(mg/L)*	K_b *(g/mg.min)*	$q_{e\ theo.}$ *(mg/g)*	$q_{e\ exp.}$ *(mg/g)*	R^2 *(%)*
30	0.006	27.21	25.19	36.2
40	0.010	33.36	30.76	88.1
50	0.006	39.24	35.74	80.6

The plot of the t/q curves as a function of time is shown in Figure 21 and the parameters of the Blanchard model are given in Table 4. The presentation of the Blanchard model gives a poor regression and the values of the theoretical maximum quantities calculated are very far from the experimental values in the three cases studied. According from these results, we conclude that the kinetics of adsorption of zinc by kaolin in aqueous medium under the optimal operating conditions is pseudo first order.

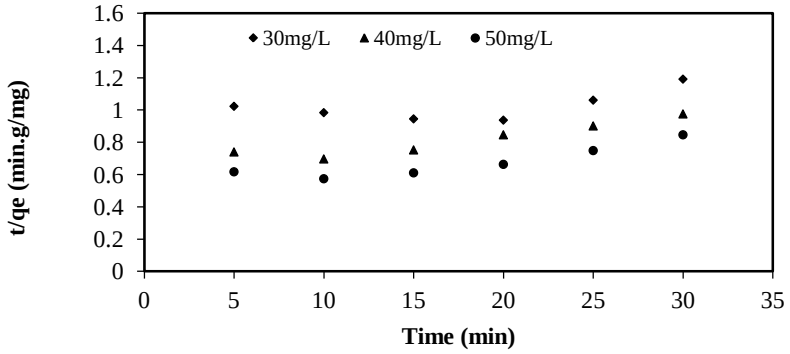

Figure 21. Pseudo second order kinetic

3.6. Adsorption mechanism

The adsorption of metals ions in solution by a solid is controlled by various steps including diffusion phenomena and fixation phases:

- diffusion of the metals ion from the solution to the boundary layer,.
- diffusion of the metals ion of the boundary layer toward the surface of the adsorbent: external transport,
- diffusion of the metals ion from the solid surface to the inside of the pores: Internal transport
- fixation of the metals ion on the adsorbent material sites

3.6.1.External transport

If the adsorption process is controlled by the external transport (resistance due to the boundary layer) the logarithm of residual concentration as a function of time must be linear function[70]. The straight-line plot from the logarithm function of the residual concentration as a function of time [lnC = f (t)], has allowed us to conclude that external transport seems to be a step controlling the speed of the overall zinc sorption process in aqueous solution by kaolin (Fig. 22). This phenomenon is justified by the results of the tests carried out, where we find that the correlation coefficients for the three-selected media and under the optimum operating conditions are greater than 0.95 (Table 5).

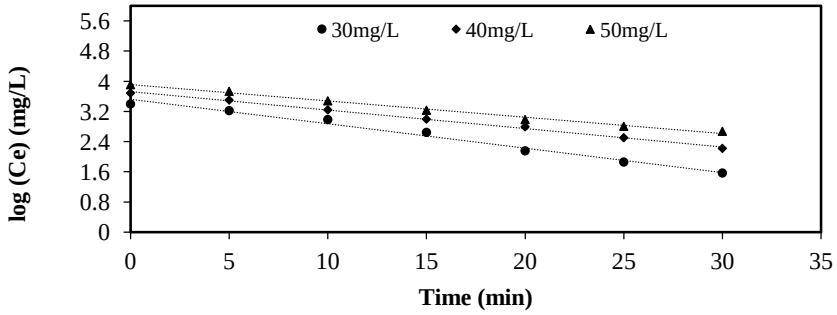

Figure 22. External diffusion kinetic for adsorption of kaolin

3.6.2. Internal transport

Weber and Morris[71] reported that if intra-particular scattering is involved in the sorption process, by increasing the adsorbed amount as a function of the square root of time, we need to obtain a line. This step is limiting if the line passes through the origin[72]. In the case where these lines do not pass through the origin, this indicates that the diffusion in the pores, but is not the only limiting mechanism of the sorption kinetics. It appears that other mechanisms are involved[73,74]. The relation of Weber and Morris is presented as follows:

$$q = k_w\sqrt{t} \quad (12)$$

Where q is quantity adsorbed at time t, t is time measured in minute, $k_{d,int}$ is the diffusion rate constant in the pores(mg/m. min ^{½}). K_w slope is defined as a speed parameter which characterizes the kinetics of adsorption in the area or the pore diffusion is the rate limiting step. The intercept indicates the effect of the boundary layer, and the greater the contribution of external diffusion in the sorption rate limitation[75,76].

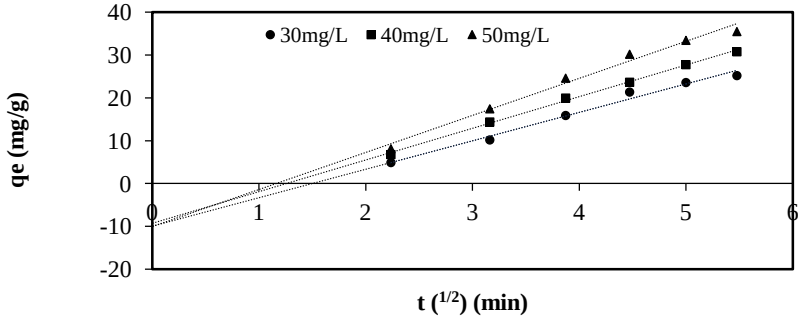

Figure 23. Intra-particle diffusion kinetic for adsorption of kaolin

According to Figure 23, we observe that the set of straight lines resulting from the function qe = f ($^{t1/2}$) doesn't pass through the origin, which shows that the diffusion of zinc into the pores is not the only mechanism limiting sorption kinetics, there are surely other mechanisms involved[77,78]. The Weber and Morris model parameters are shown in Table 5.

Table 5. Values of internal and external transport parameters

	Weber et Morris parameters			External transport parameters
C_0 *(mg/L)*	***The intercept***	R^2 %	k_w *(mg/g.min)*	R^2%
30	6.63	98.4	5.43	98.5
40	7.38	99.1	6.44	99.6
50	8.65	98.4	7.69	99.2

3.7 Thermodynamic study

The thermodynamic parameters of zinc sorption by kaolin can be related to the distribution coefficient (kc) by the following equation[79,80]:

$$\Delta G^0 = -RTlnk_c \quad (13)$$

Where R is perfect gas constant, T is Temperature in kelvin (K), K_c is Coefficient of distribution (L/g).

We know from the laws of thermodynamics of solutions that the variation of the free enthalpy is given by the following equation (14):

$$\Delta G^0 = \Delta H^0 - T\Delta S^0 \quad (14)$$

hence, we will deduce the following equation

$$lnk_c = \frac{\Delta H^0}{R} \times \frac{1}{T} + \frac{\Delta S^0}{R} \quad (15)$$

By plotting the logarithm of the distribution coefficient kc as a function of the inverse of the temperature [lnkc = f (1 / t)], we obtain a line which allows us to determine in the first-place enthalpy. The entropy ΔS^0 is calculated by the equation below (eq. 16)

$$\Delta S^0 = -\frac{\Delta G^0 - \Delta H^0}{T} \quad (16)$$

The solute distribution coefficient is calculated from equation 17[81-83].

$$k_c = \frac{C_i - C_e}{C_e} \times \frac{V}{M} = \frac{q_e}{C_e} \quad (17)$$

Table 6. Values of the distribution coefficient at different temperatures

T*(K)*	293	303	313	323
k_c *(L/g)*	1.911	1.626	1.369	0.99

Table 7. Thermodynamic parameters for the adsorption of kaolin

Temperature *(K)*	293	303	313	323
ΔH^0 *(kj/mole)*	-13.379			
ΔG^0 *(kj/mole)*	-4.647	-4.091	-3.561	-2.738
ΔS^0 *(j/mole.K)*	-40.20			

The values of the distribution coefficient k_c are reported in table 6, the values of the thermodynamic parameters are presented in Table 7 and the line from the function lnkc = f (1 / T) is shown in Figure 24. Table 7 shows the following effects:

- the negative values of ΔG^0 indicate that the adsorption process is spontaneous[84,85],
- the absolute value of ΔG^0 decreases with the temperature increase which shows that the adsorption is favored at low temperature [86,87],
- the negative value of ΔH^0shows that the adsorption process is exothermic[88,89],
- the negative value of ΔS^0 reveals that the randomness of zinc adsorption by kaolin has decreased at the solid/solution interface[90-92] and the adsorption process is energetically stable [93].

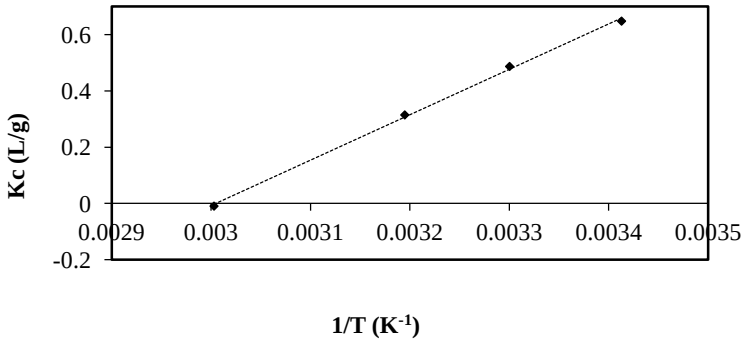

Figure 24. Van't Hoff linear plot of lnkc vs. 1/T

4. Conclusion

The characterization study of kaolin showed that it consists mostly of alumina, silica and a small amount of quartz. It also indicated that its structure is disordered and the zero-point charge (PZC) of the kaolin, determined by pH measurements was 6.6.The kinetic study allowed us to conclude that the adsorption of zinc in solution by kaolin is feasible, where the yield is maximum (83.9%) for the low concentrations. The pseudo equilibrium is reached after 30 minutes and the maximum capacity of adsorbed zinc is 39.39 mg / g. This sorption phenomenon follows pseudo first-order kinetics and obeys Langmuir model. The affinity ratio R_L showed that kaolin has a high adsorption capacity. The Freundlich constant (n> 1) reveals that the adsorption is favorable. The study of the adsorption mechanism shows that external transport seems to be a step controlling the speed of the overall process of zinc sorption in solution. However the diffusion into pores is not the only mechanism limiting the sorption kinetics. The thermodynamic study showed that this process is spontaneous, exothermic and the fixation of zinc by the kaolin did not change its structure.

Références

1. S.A. Nabi, R. Bushra, Z.A. Al-Othman, Mu. Naushad, Synthesis, characterization and analytical applications of a new composite cation exchange material acetonitrile stannic(IV) selenite: adsorption behavior of toxic metal ions in nonionic surfactant medium, Sep. Sci. Technol. 46 (2011) 847–857.
2. M. Ozmen, K.Can, G. Arslan, A. Tor, M. Ersoz, Adsorption of Cu(II) from aqueous solution by using modified Fe_3O_4 magnetic nanoparticles, Desalination 254 (2010) 162-169.
3. F. Testard, L. Berthon , A. Thomas, Liquid–liquid extraction: An adsorption isotherm at divided interface. C. R. Chim. 10 (2007) 1034-1041.
4. A. Efligenir, S. Déon, P. Fievet, C. Druart, G. Crini, Decontamination of polluted discharge waters from surface treatment industries by pressure-driven membranes: Removal performances and environmental impact. Chem. Eng. J. 258 (2014) 309-319.

5. K. Trivunac, S. Stevanovic, Removal of heavy metal ions from water by complexation-assisted ultrafiltration, Chemosphere 64 (2006) 486-491.
6. B. Taraba, P. Bulavová, Adsorption enthalpy of lead(II) and phenol on coals and activated carbon in the view of thermodynamic analysis and calorimetric measurements, The J. Chem. Thermodyn., 116 (2018) 97-106.
7. S. Agarwal, I. Tyagi, V.K. Gupta, A.R. Bagheri, A.A. Bazrafshan, Rapid adsorption of ternary dye pollutants onto copper (I) oxide nanoparticle loaded on activated carbon: Experimental optimization via response surface methodology, J. Environ. Chem. Eng., 4 (2016) 1769-1779.
8. L. Mouni, L. Belkhiri, J.C. Bollinger, A. Bouzaza, A. Assadi, A. Tirri, F. Dahmoune, K. Madani, H. Remini, Removal of Methylene Blue from aqueous solutions by adsorption on Kaolin: Kinetic and equilibrium studies, Appl. Clay Sci., 153 (2018) 38-45
9. G.S. Gupta, S.P. Shukla, G. Prasad, V.N. Singh, China clay as an adsorbent for dye house wastewaters. Environ. Technol., 13 (1992) 925-936.
10. V. Vimonses, S. Lei, B. Jin, Chris W.K. Chow, C. Saint, Adsorption of congo red by three Australian kaolins, Appl. Clay Sci., 43 (2009) 465-472
11. B.K. Nandi, A. Goswami, M.K Purkait, Removal of cationic dyes from aqueous solutions by kaolin: Kinetic and equilibrium studies, Appl. Clay Sci., 42(2009) 583-590
12. S. Wang, L. Alagha, Z. Xu, Adsorption of organic–inorganic hybrid polymers on kaolin from aqueous solutions, Colloids and Surfaces A: Physicochemical and Eng. Aspects, 453 (2014) 13-20
13. R.G. Harris, J.D. Wells, B.B. Johnson, Selective adsorption of dyes and other organic molecules to kaolinite and oxide surfaces. Colloids Surf., A Physicochem. Eng. Asp. 180 (2001) 131 140.
14. Z. Dali-Youcef, H. Bouabdasselem, N. Bettahar, Élimination des composés organiques par des argiles locales, C. R. Chim., 9 (2006) 1295-1300
15. Z. Danková, A. Bekényiová, I. Štyriaková, E. Fedorová, Study of Cu(II) Adsorption by Siderite and Kaolin, Procedia Earth and Planetary Sci., 15 (2015) 821-826
16. M. Arias, M.T. Barral, J.C. Mejuto, Enhancement of copper and cadmium adsorption on kaolin by the presence of humic acids, Chemosphere, 48 (2002) 1081-1088.
17. C. Huang, Y.L. Yang, Adsorption characteristics of Cu(II) on humus-kaolin complexes. Water Res. 29(1995) 2455-2460
18. Y. Chammui, P. Sooksamiti, W. Naksata, S. Thiansem, Orn-anong Arqueropanyo, Removal of arsenic from aqueous solution by adsorption on Leonardite, Chem. Eng. J., 240 (2014) 202-210
19. K.O. Adebowale, I.E. Unuabonah, B.I. Olu-Owolabi, Adsorption of some heavy metal ions on sulfate- and phosphate-modified kaolin. Appl. Cla. Sc. 29 (145-148) 2005.
20. K.O. Adebowale, E. Unuabonah, B.I. Olu-Owolabi, I. Bamidele, The effect of some operating variables on the adsorption of lead and cadmium ions on kaolinite Clay. J. Hazard. Mater. B134 (2006) 130-139.
21. E.I. Unuabonah, K.O. Adebowale, B.I. Olu-Owolabi, L.Z. Yang, L.X. Kong, Adsorption of Pb (II) and Cd (II) from aqueous solutions onto sodium tetraborate-modified Kaolinite clay: Equilibrium and thermodynamic studies. Hydrometallurgy 93 (2008) 1-9.
22. C. R. Burch, Mesoporous materials for water treatment processes, Water Res. 33 (199) 3689-3694.
23. Norme afnor NF T 90-112, Essais des eaux - Dosage de dix éléments métalliques (Cr, Mn, Fe, Co, Ni, Cu, Zn, Ag, Cd, Pb) par spectrométrie d'absorption atomique avec flamme
24. S. Brunauer, P.H. Emmet, E. Teller, Adsorption of gases in multimolecular layers, J. Amer. Chem. Soc. 60 (1938),309.
25. Z.A. AL-Othman, R. Ali, Mu. Naushad, Hexavalent chromium removal from aqueous medium by activated carbon prepared from peanut shell: Adsorption kinetics, equilibrium and thermodynamic studies, Chem. Eng. J. 184 (2012) 238- 247
26. M.E. Fernandez, B. Ledesma, S. Roman, P.R. Bonelli, A.L. Cukierman, Development and characterisation of activated hydrochars from orange peels as adsorbents for emerging organic contaminants, Bioresour. Technol. 183 (2015) 221-228.
27. L. Dinga, B. Zoua, W. Gaob, Q. Liua, Z. Wanga, Y. Guoa, X. Wanga, Y. Liuaa, Colloids and Surfaces A: Physicochem. Eng. Aspects 446 (2014) 1-7
28. P. Chutia, S. Kato, T. Kojima, S. Satokawa, J. Hazard. Mater. 162 (2009) 440-447
29. M. Saranya, S. Latha, M.R GopalReddi., T. Gomathi, S. Anil. Adsorption Studies of Lead(II) from aqueous solution onto Nanochitosan /Polyurethane /Polypropylene glycol ternary blends. Int J. Biol. Macromolec. 16 (2017) 436-1448.

30. M. Haerifar, S. Azizian, Fractal-like adsorption kinetics at the solid/solution interface, J. Phys. Chem. 116 (2012) 13111-13119.
31. D. Park, Y.S. Yun, J.M. Park, The past, present, and future trends of biosorption, Biotechnol. Bioprocess. Eng.15 (2010) 86-102.
32. T. Jiang, W. Liu, Y. Mao, L.Zhang, J. Cheng, M.Gong, H. Zhao, L. Dai, S. Zhang, Q. Zhao. Adsorption behavior of copper ions from aqueous solution onto graphene oxide–CdS composite. Chem. Eng. J. 259 (2015) 603-610.
33. A. Labidi , A. M. Salaberria , S. C.M. Fernandes , J. Labidi, M. Abderrabba. Adsorption of copper on chitin-based materials: Kinetic and thermodynamic studies, J. Tai. Inst. Chem. Eng. 65 (2016) 140-148.
34. T.V. Bauer, T.M. Minkina, D.L. Pinskii, S.S. Mandzhieva, S.N. Sushkova, Adsorption of copper by ordinary and southern chernozems from solutions of different salts, J. Geochem. Explor.176 (2017) 108-113.
35. H. Demiral, C. Güngör. Adsorption of copper(II) from aqueous solutions on activated carbon prepared from grape bagasse, J. Clean. Prod.124, 15 (2016) 103-113.
36. T. Chouchane, M. Yahi, A. Boukari, A. Balaska, S Chouchane., Adsorption of the copper in solution by the kaolin, J. Mater. Environ. Sci. 7 (2016) 2825-2842
37. Bakhtiari, S. Azizian, Adsorption of copper ion from aqueous solution by nanoporous MOF-5: A kinetic and equilibrium study, J. Molec. Liqui.206 (2015) 114-118
38. S. Comte, G. Guibaud, M. Baudu, Biosorption properties of extracellular polymeric substances (EPS) towards Cd, Cu and Pb for different pH values, J. Hazard. Mater. 151 (2008) 185–193.N.
39. M. Wiśniewska, K. Szewczuk-Karpisz, I. Ostolska, Temperature effect on the adsorption equilibrium at the silica–polyethylene glycol solution interface, Fluid. Phase Equilib.360 (2013) 10-15.
40. T. M. Berhane, J. Levy, Mark P.S. Krekeler, N. D. Danielson, Adsorption of bisphenol A and ciprofloxacin by palygorskite-montmorillonite: Effect of granule size, solution chemistry and temperature, App. Clay. Sc. 132–133 (2016) 518-527.
41. P.S. Kumar, S. Ramalingam, S. Dinesh Kirupha, A. Murugesan, T. Vidhyadevi, S. Sivanesan, Adsorption behavior of nickel(II) onto cashew nut shell: Equilibrium, thermodynamics, kinetics, mechanism and process design , Chem. Eng. J. 167 (2011) 122-131.
42. C. Hu, P. Zhu, M. Cai, H. Hu, Q. Fu. Comparative adsorption of Pb(II), Cu(II) and Cd(II) on chitosan saturated montmorillonite: Kinetic, thermodynamic and equilibrium studies, App. Clay Sc.143(2017) 320-326.
43. W.S. Wan Ngah, M.A.K.M. Hanafiah, Adsorption of copper on rubber (Heveabrasiliensis) leaf powder: Kinetic, equilibrium and thermodynamic studies Biochem. Eng. J. 39 (2008) 521-530.
44. M. Sekar, V. Sakthi, S. Rengaraj, Kinetics and equilibrium adsorption study of lead(II) onto activated carbon prepared from coconut shell, J. Coll. Interf. Sc. 279 (2004) 307-313
45. Y. Matsui, S Nakao, A. Sakamoto, T. Taniguchi, N. Shirasaki. Adsorption capacities of activated carbons for geosmin and 2-methylisoborneol vary with activated carbon particle size: Effects of adsorbent and adsorbate characteristics Water Res. 85 (2015) 95-102
46. B. Chen, W. Sun, C. Wang, X. Guo, Size-dependent impact of inorganic nanoparticles on sulfamethoxazole adsorption by carbon nanotubes, Chem. Eng. J.316 (2017) 160-170.
47. D. Satapathy, G. S. Natarajan, Potassium bromate modification of the granular activated carbon and its effect on nickel adsorption, Ads. 12 (2006) 147-154.
48. A.S. Ozcan, A. Ozcan, Adsorption of acid dyes from aqueous solutions onto acid-activated bentonite, J. Coll. and Interf. Sc. 276 (2004) 39-46.
49. K.G. Bhattacharyya, S.S. Gupta, Adsorption of Fe (III) from water by natural and acid activated clays: studies on equilibrium isotherm, kinetics and thermodynamics of interactions, Ads. 12 (2006) 185-204.
50. J.P. Chen, S. Wu, K.H. Chong, Surface modification of a granular activated carbon by citric acid for enhancement of copper adsorption, Carbon 41 (10) (2003) 1979-1986.
51. L.A. Romero-Cano, H. García-Rosero, L.V. Gonzalez-Gutierrez, L.A. Baldenegro-Pérez, F. Carrasco-Marín, Functionalized adsorbents prepared from fruit peels: Equilibrium, kinetic and thermodynamic studies for copper adsorption in aqueous solution, J. Clea. Prod.162, (2017) 195-204.
52. H. Demiral, C. Güngör, Adsorption of copper(II) from aqueous solutions on activated carbon prepared from grape bagasse, J. Clea. Prod.124 (2016), 103-113
53. H.M.F. Freundlich, Over the Adsorption in Solution, J. Phys. Chem. 57 (1906) 385-470.

54. I. Langmuir, The adsorption of gases on plane surfaces of glass, mica and platinum, J. Am. Chem. Soc. 40 (1918) 1361-1403.
55. C. Ng, J.N. Losso, W.E. Marshall, R.M. Rao, Freundlich adsorption isotherms of agricultural by-product-based powdered activated carbons in a geosmin–water system, Bioresour. echnol. 85 (2002) 131-135.
56. F.Y. Sun, J.L. Chen, A.M. Li, F.Q. Liu, Q.X. Zhang, Adsorption of phenol from aqueous solution by aminatedhypercrosslinked polymers, Ads. Sci. Technol. 23 (2005) 335-345.
57. S. Veli, B. Pekey, Removal of copper from aqueous solution by ion exchange resins Fresenius Environ. Bull. 13 (2004) 244-250.
58. M. Torab-Mostaedi, M. Asadollahzadeh, A. Hemmati, A. Khosravi. Equilibrium, kinetic, and thermodynamic studies for biosorption of cadmium and nickel on grapefruit peel, J. Tai. Inst. Chem. Eng. 44 (2013) 295–302.
59. F. Y. Wang, H. Wang, J. W. Ma, Adsorption of cadmium (II) ions from aqueous solution by a new low-cost adsorbent—Bamboo charcoal, J. Hazard. Mater. 177 (2010) 300-306.
60. W.S.W. Ngah, S. Fatinathan, Adsorption characterization of Pb(II) and Cu(II) ions onto chitosan-tripolyphosphate beads: kinetic, equilibrium and thermodynamic studies, J. Environ. Manage. 91 (2010), 958–969.
61. J.P. Maran, V. Sivakumar, R. Sridhar, K. Thirugnanasambandham. Development of model for barrier and optical properties of tapioca starch based edible films, Carbohydr. Polym. 92 (2013) 1335-1347.
62. Y. B. Onundi, A. A. Mamun, M. F. Al Khatib, Y. M. Ahmed. Adsorption of copper, nickel and lead ions from synthetic semiconductor industrial wastewater by palm shell activated carbon. Int. J. Environ. Sci. Technol. 7 (2010) 751-758.
63. I. Lakhdhar, P. Mangin, B. Chabot. Copper (II) ions adsorption from aqueous solutions using electrospun chitosan/peonanofibres: Effects of process variables and process optimization, J. Water Proc. Eng. 7 (2015), 295-305.
64. M. Abdel Salam, G. Al-Zhrani , S.A. Kosa, Simultaneous removal of copper(II), lead(II), zinc(II) and cadmium(II) from aqueous solutions by multi-walled carbon nanotubes, C. R. Chim. 15 (2012), 398-408
65. P.E.P. Barrett, L.G. Joyner, P.P. Halenda, The Determination of Pore Volume and Area Distributions in Porous Substances. I. Computations from Nitrogen Isotherms, J. Am. Chem. Soc. 73 (1951) 373–380.
66. M. Haerifar, S. Azizian, Fractal-Like Kinetics for Adsorption on Heterogeneous Solid Surfaces, J. Phys. Chem. C 118 (2014) 1129-1134.
67. M. Ghaedi, E. Shojaeipour, A.M. Ghaedi, R. Sahraei, Isotherm and kinetics study of malachite green adsorption onto copper nanowires loaded on activated carbon: Artificial neural network modeling and genetic algorithm optimization . Acta A: Mol. Biomol. Spectros. 142 (2015a), 135-149.
68. K. Vijayaraghavan, T.V.N. Padmesh, K. Palanivelu, M. Velan, Biosorption of nickel(II) ions onto Sargassumwightii: Application of two-parameter and three-parameter isotherm models, J. Hazard. Mat. 133 (2006) 304-309.
69. I. Ullah, R. Nadeem, M. Iqbal, Q. Manzoor, Biosorption of chromium onto native andimmobilized sugarcane bagasse waste biomass, Ecol. Eng. 60 (2013) 99-107.
70. D.M. Nevshia, A. Santianes, V. Munoz, A. Guerrero-Ruizi,. Interaction of aqueous solutions of phenol with commercial actived carbons as adsorption and kinetic study,Carbon 37(1995) 1065-1074.
71. W.J. Weber, J.C. Morris, Kinetics of adsorption on carbon from solution, J. Sanit. Eng. Div. Am. Soc. Civ. Eng. 89 (1963) 3-60.
72. E. Asuquo, A. Martin, P. Nzerem, F. Siperstein, X. Fan, Adsorption of Cd(II) and Pb(II) ions from aqueous solutions using mesoporous activated carbon adsorbent: Equilibrium, kinetics and characterisation studies, J. Environ. Chem. Eng., 5 (2017) 679-698
73. H. Demiral, C. Güng. Adsorption of copper(II) from aqueous solutions on activated carbon prepared from grape bagasse, J. Clea. 124 (2016) 103-113.
74. P. Senthil Kumar, S. Ramalingam, S. Dinesh Kirupha, A. Murugesan, T. Vidhyadevi, S. Sivanesan, Adsorption behavior of nickel(II) onto cashew nut shell: Equilibrium, thermodynamics, kinetics, mechanism and process design, Chem. Eng. J. 167 (2011) 122-131.
75. A.T. Mohd Din, B.H. Hameed, A.L. Ahmad, Batch adsorption of phenol onto physiochemical-activated coconut shell, J. Hazard. Mater. 161 (2009) 1522-1529.
76. M.F. Taha, C.F. Kiat, M.S. Shaharun, A. Ramli, World Acad. Sci. Eng. Tech. 60 (2011).
77. R.S. Azarudeen, M.A.R. Ahmed, R. Subha, A.R. Burkanudeen, Heavy and toxic metal ion removal by a novel polymeric ion-exchanger: synthesis, characterisation, kinetics and equilibrium, J. Chem. Technol. Biotechnol. 90 (2015) 2170-2179.

78. A. Gurses, A. Hassani, M. Kıransan, O. Acıslı, S. Karaca, Removal of methylene blue from aqueous solution using by untreated lignite as potential low-cost adsorbent: kinetic, thermodynamic and equilibrium approach, J. Water Process Eng. 2 (2014) 10-21.
79. M.A. Badawi, N.A. Negm, M.T.H. Abou Kana, H.H. Hefni, M.M. Abdel Moneem, Adsorption of aluminum and lead from wastewater by chitosan-tannic acid modified biopolymers: Isotherms, kinetics, thermodynamics and process mechanism,Int. J. Biolog.Macromol. 99 (2017) 465-476.
80. F. Bouhamed, Z. Elouear, J. Bouzid, Adsorptive removal of copper(II) from aqueous solutions on activated carbon prepared from Tunisian date stones: Equilibrium, kinetics and thermodynamics, J. Tai. Inst. Chem. Eng. 43 (2012) 741-749.
81. T. Chouchane, S. Chouchane, A. Boukari, A. Mesalhi, J. Mater. Environ. Sci. 6 (2015) 924-941.
82. M. Mushtaq, H.N. Bhatti, M. Iqbal, S. Noreen, Eriobotrya japonica seed biocomposite efficiency for copper adsorption: Isotherms, kinetics, thermodynamic and desorption studies; J. Environ. Manage. 176 (2016) 21-33.
83. J. Zhu, M. Dai, S. He, Q.L. Gong, Renmin, Cationic surfactant hemimicelle on alginate gel for removing bisphenol A from aqueous solution, Desalination & Water Treatment, 52(22) (2014) 4388-4394.
84. A. Adamczuk, D. Kołodyńska, Equilibrium, thermodynamic and kinetic studies onremoval of chromium, copper, zinc and arsenic from aqueous solutions onto fly ashcoated by chitosan Chem. Eng. J. 274(2015) 200-212.
85. M. Akram, H. Nawaz Bhatti, M. Iqbal, S.Noreen, S. Sadaf. Biocomposite efficiency for Cr(VI) adsorption: Kinetic, equilibrium and thermodynamics studies, J.Environ.Chem.Eng, V 5 (2017), 400-411
86. M. Fouodjouo, H. Fotouo-Nkaffo, S. Laminsi, F.A. Cassini, L. O. Brito-Benetoli, N.A. Debacher, Adsorption of copper (II) onto cameroonian clay modified by non-thermal plasma: Characterization, chemical equilibrium and thermodynamic studies, Applied Clay Science, 142 (2017) 136-144
87. X. J. Hu, J. S. Wang, Y. G. Liu, X. Li, G. M. Zeng, Z. L. Bao, F. Long, Adsorption of chromium (VI) by ethylenediamine-modified cross-linked magnetic chitosan resin: isotherms, kinetics and thermodynamics, J. Hazard. Mater. 185 (2011) 306-314
88. I. Belbachir, B. Makhoukhi, Adsorption of Bezathren dyes onto sodicbentonite from aqueous solutions, J.Tai.Inst. Chem. Eng., 75 (2017) 105-111.
89. C. Hu, P. Zhu, M.Cai, H. Hu, Q. Fu, Comparative adsorption of Pb(II), Cu(II) and Cd(II) on chitosan saturated montmorillonite: Kinetic, thermodynamic and equilibrium studies, App. Clay Sc. 143 (2017) 320-326
90. Manasi, V. Rajesh, N. Rajesh. Adsorption isotherms, kinetics and thermodynamic studies towards understanding the interaction between a microbe immobilized polysaccharide matrix and lead, Chem. Eng. J. 248 (2014) 342-351.
91. A. Olgun, N. Atar, Equilibrium, thermodynamic and kinetic studies for the adsorption of lead (II) and nickel (II) onto clay mixture containing boron impurity , J. Ind. Eng. Chem. 18 (2012) 1751-1757
92. C. Gerente, V.K.C. Lee, C. P. Le, G. McKay, Application of chitosan for the removal of metals from wastewaters by adsorption-mechanisms and models review, Crit. Rev. Environ. Sci. Technol. 37 (2007) 41-127.
93. Y. Wu, H. Luo, H. Wang, C. Wang, J. Zhang, Z. Zhang, Adsorption of hexavalentchromium from aqueous solutions by graphene modified with cetyltrimethylammonium bromide, J. Colloid Interface Sci. 394 (2013) 183-191.